A Mathematical Model for Estimating the Effective Thermal Conductivity of Photonic Crystal Fiber Cladding with Honeycomb Lattice Structure

Maryam Karimi

Faculty Member of Photonic and Quantum Technology Research School, Nuclear Science and Technology Research Institute, AEOI, Tehran, Iran.

Corresponding Author Email: mykarimi@aeoi.org.ir

Received: June 20, 2026, Revised: Ja. 24, 2026, Accepted: Feb. 01, 2026, Available Online: Feb. 03, 2026,
DOI: Due to the current conditions, there is no possibility to buy DOI for papers. We hope to buy them as soon as possible.

ABSTRACT— This study introduces a novel analytical model for estimating the effective thermal conductivity of photonic crystal fibers (PCFs) with a honeycomb lattice cladding. This innovative model allows for the estimation of thermal conductivity across layers and the entire honeycomb structure for a wide range of hole diameters and inter-hole spacings, eliminating the need for specialized simulation software. As an analytical model, it offers higher computational accuracy compared to previous methods. Unlike triangular lattices, the modeling process explicitly considers the two distinct unit cell types inherent to the honeycomb lattice.

Using the proposed method, we evaluated the thermal conductivity of honeycomb-structured PCFs for various hole sizes and pitches. Results indicate that thermal conductivity stabilizes with an increasing number of layers, and the air filling fraction plays a dominant role in thermal performance, leading to a significant reduction in conductivity. This work enables the rapid optimization of PCFs for high-power laser applications (e.g., Air-Si PCFs) and low-loss sensors (e.g., H_2-ZBLAN PCFs), with direct implications for thermal stability in optical systems.

KEYWORDS: Thermal Conductivity Coefficient, Honeycomb Structure, Mathematical Model, Thermal Resistance.

I. INTRODUCTION

Honeycomb structures have gained increasing attention in recent decades due to their superior mechanical strength, lightweight nature, and high surface-area-to-volume ratio, making them ideal for applications involving mechanical loading, impact resistance, and thermal management [1–3]. Their geometric stability and natural occurrence at both micro- and nano-scales make them especially attractive in biological systems and engineered materials [4, 5].

Honeycomb structures are increasingly used in engineering constructions subjected to dynamic stresses, including earthquakes, explosions, and strong winds [6], mechanical systems [7], energy-absorbing panels [8], chemical engineering [9], and materials science [10]. The mechanical robustness and efficient thermal conduction paths within honeycomb geometries make them suitable for demanding operational environments. Recent studies have also utilized honeycomb porous networks in polymer thin films [11], activated carbon scaffolds [12], and metallic or ceramic cellular structures [13].

In the domain of photonics, honeycomb-lattice photonic crystal fibers (PCFs) have demonstrated potential for enhanced mode control, dispersion engineering, and heat dissipation [14]–[17]. Compared to conventional triangular lattice PCFs, the honeycomb arrangement involves two distinct unit cell geometries, introducing analytical

challenges in modeling their thermal performance.

Although several numerical and semi-analytical methods have been proposed to evaluate thermal conductivity in porous and composite media [18-22], there is a growing demand for lightweight, analytical tools that can estimate the effective thermal conductivity of such complex structures with minimal computational overhead.

In this paper, we propose an analytical model based on thermal resistance networks to determine the effective thermal conductivity of PCFs with honeycomb-lattice claddings. The model accounts for geometrical variations in hole size and spacing, offering high-accuracy results without reliance on specialized numerical simulation tools.

II. Modeling the Effective Thermal Conductivity of Photonic Crystal Fibers with Honeycomb Cladding Geometry

Figure 1 shows a PCF cladding with Honeycomb Lattice Structure. In reference [7], a method for determining the effective thermal conductivity of a hexagonal unit cell along different orientations with respect to the heat flux direction is presented.

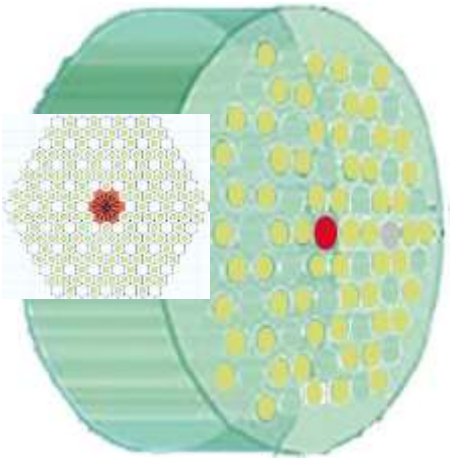

Fig. 1. PCF cladding with Honeycomb Lattice Structure and heat flux direction.

The honeycomb structure consists of two types of unit cells that illustrated in Fig. 2: those with holes and those without. The hole-free unit cells can be modeled as a single thermal resistance characterized by the thermal conductivity of the glass material. The total area of a unit cell is depending solely on the spacing between holes. On the other hand, the unit cells containing holes are composed of two materials—glass and air—which requires calculating an equivalent thermal resistance that accounts for both phases. To determine the effective thermal conductivity of these hole-containing unit cells, the cell is divided into five thermal resistances connected in a network that forms an equivalent thermal circuit.

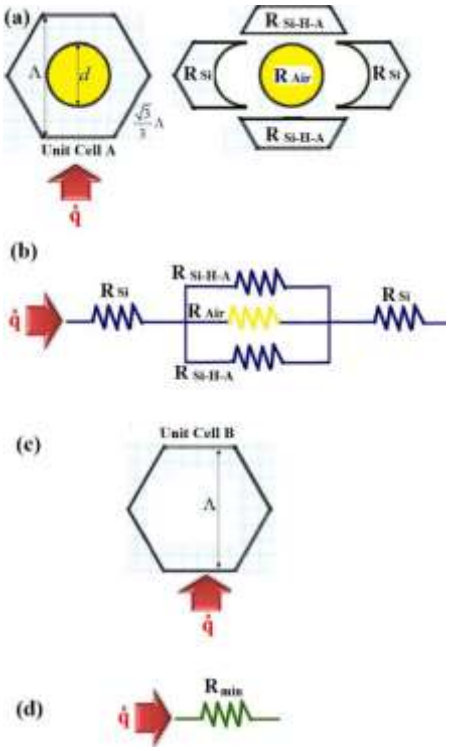

Fig. 2. Two types of Unit cells a, with, c, without hole. equivalent thermal resistance network, at unit cell b- with, d, without hole.

The effective thermal conductivity of a unit cell is calculated using the following relationship [23]:

$$\frac{L_{eff-cell}}{k_{eff-cell}S_{cell}} = \frac{2L_{Si-1}}{k_{Si}S_{Si-1}} + \frac{L_{H-A}}{k_{H-A}S_{H-A}}, \quad (1)$$

where S_{Si-1} represents the triangular area portions at the top and bottom of the hole-containing unit cell; S_{H-A} and S_{cell} denote the middle area and the total area of the hole-containing unit cell, respectively. For the case

where the heat flux is applied perpendicularly to the unit cell, the total cell area equals $S_{cell} = \sqrt{3}\Lambda^2/2$, and the hole area is $S_{H-A,1} = \sqrt{3}d\left(4\Lambda - d\right)/6$. The lengths L_{Si-1} , L_{H-A} , and $L_{eff-cell}$ correspond to the lengths of the triangular region, the middle region S_{Si-H-A} (equal to the hole diameter '*d*'), and the effective length of the unit cell Λ, respectively. The thermal conductivities k_{Si} , k_{H-A} , and $k_{eff-cell}$ denote the thermal conductivity of the glass material, the hole (air), and the effective thermal conductivity of the hole-containing unit cell, respectively. Reference [7] thoroughly explains the methodology for determining the effective thermal conductivity of the hole-containing unit cell. In the honeycomb lattice, the arrangement of unit cells in the first layer resembles a triangular lattice. In other wards the first layer of the honeycomb lattice consisting of six hole-containing unit cells and the equivalent thermal resistance circuit of the first layer has six identical resistors. However, in the second layer, the hole-containing unit cells alternate with hole-free unit cells. Figure 3(a) illustrates an example of the second layer of unit cells, while Fig. 3(b) depicts the equivalent thermal resistance circuit of this layer.

The thermal resistance of the second layer consists of six thermal resistances from the hole-containing unit cells connected in parallel with six thermal resistances from the hole-free unit cells. Other layers in the structure follow a similar configuration and are divided in the same manner. The equivalent thermal resistance circuit model is designed such that each part of the unit cell—including glass and air sections—is represented by separate resistances connected in series and parallel arrangements. This model allows researchers to easily analyze the effects of variations in hole size and spacing and predict their impact on the overall effective thermal conductivity of the structure. In the equivalent thermal-resistance network, each resistor represents a specific radial segment of the PCF cladding characterized by its own geometry and thermal conductivity. the thermal resistance of each section is first computed individually, and then the total effective resistance of the cross-section is evaluated using appropriate series and parallel combinations according to the physical configuration of the glass and air regions.

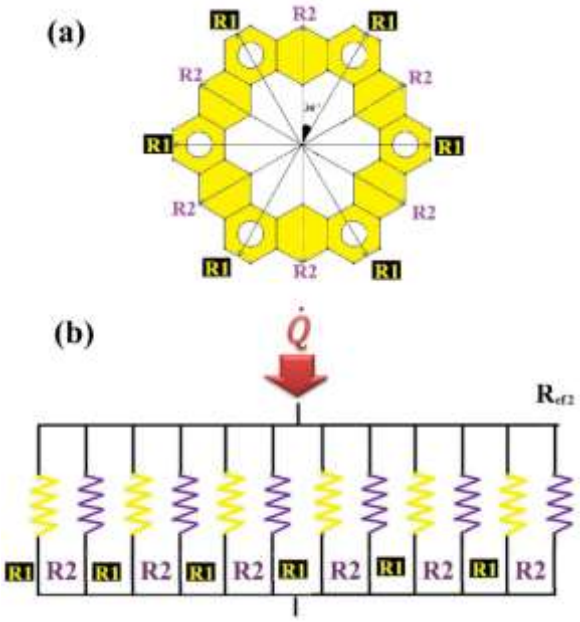

Fig. 3. (a) The second layer of the honeycomb, (b) Equivalent thermal resistance circuit of the second layer.

Furthermore, this model can be applied in thermal simulations of the entire photonic crystal fiber with a honeycomb cladding structure, where heat transfer from the fiber core to the cladding is of particular importance. Therefore, having an accurate and computationally efficient analytical model for the effective thermal conductivity can aid in optimizing fiber designs and improving their thermal performance.

The total thermal resistance of parallel elements is calculated using the following relation:

$$\frac{1}{R_{eff-layer(n)}} = \sum_{i=1}^{6n} \frac{1}{R_{eff-cell(i)}}, \tag{2}$$

where $R_{eff-cell-i}$ is the thermal resistance of the ith hole-containing unit cell. The most influential parameter affecting the effective thermal resistance value is the radius of the hole. As the hole radius increases, the effective thermal resistance approaches the thermal resistance value of the material that fills the

hole (i.e., air). Each layer consists of 6n unit cells. In a triangular lattice, all unit cells contain holes, whereas in the honeycomb lattice, a combination of hole-containing and hole-free unit cells is present. All unit cells in every layer—whether with or without holes—are connected in parallel. The calculation of the effective thermal conductivity for the ith layer depends on the layer number, unlike the triangular lattice where only one computational case exists.

The resistance of each individual unit cell is itself an effective value, calculated from its internal series-parallel network of glass and air segments (as shown in Figs. 2(b) and 2(d), and depends on its specific orientation within the lattice [24].

In the honeycomb lattice, three distinct cases arise depending on the numerical value of n (the layer number). The effective thermal conductivity for these three cases is calculated as follows. If the layer number n+2 is a multiple of three, or equivalently for n+2=3k, or in other words $n=\{4,7,10,13,16,19,22,25,28,...\}$, then the effective thermal conductivity is determined by:

$$k_{eff-layer-n} = \frac{k}{n}k_{m1} + \sum_{i=1}^{k}\frac{2}{n}k_{cell}\left(\theta=\frac{t\pi}{3n}\right) + \frac{1}{n}k_{cell}\left(\theta=0\right), \quad (3)$$

The honeycomb lattice exhibits a periodic pattern in the sequence of unit cell types (with and without holes) across consecutive layers. Equation 3 provides a generalized analytical expression for the layer's effective conductivity, derived by applying the parallel resistance model to this repeating pattern. In this case $t=2,5,8,11,14,17,20,...$ and t is a real number. If the layer number n is a multiple of three, i.e., $n=\{3,6,9,12,15,18,21,24,30\}$, then t in Eq. (3), is $t=3,6,9,12,15,18,...$ n is odd. If the layer number n+1 is a multiple of three, i.e., $n=\{2,5,8,11,14,17,20,23,26,29,...\}$, then the maximum value between k and k−1 is swapped and $t=1,4,7,10,13,16,19,$.

Each layer has its own effective thermal conductivity, and the overall effective thermal resistance of the honeycomb lattice network is obtained by summing the resistances of the individual layers. Along the direction of heat flux propagation, the layers are connected in series; thus, the total effective thermal resistance is $R_{Total}=\sum_{i=1}^{n}R_{eff-layer-i}$. where $R_{eff-layer-i}$ is the effective thermal resistance of the ith layer and R_{Total} is total thermal resistance of honeycomb lattice structure. In reference [7], a one-dimensional model and radial heat propagation are assumed. Therefore, Fourier's law for cylindrical surfaces is not considered, which introduces computational errors at the macroscale. To improve this computational approach, instead of assuming heat transfer in a planar layer, heat transfer is modeled in cylindrical layers with different thermal conductivity coefficients.

The thermal resistance of a cylinder with length L, inner radius r_1, and outer radius r_2 is expressed as $R_{Clyn}=Ln\left(r_2/r_1\right)/2\pi K_{layer}L$ [7]. Accordingly, the effective thermal conductivity of the honeycomb structure is given by:

$$k_{Total}=\left[\frac{1}{Ln(n+1)}\sum_{i=1}^{n}\frac{Ln\left(\frac{n+1}{n}\right)}{k_{eff-layer-i}}\right]^{-1}, \quad (4)$$

where n is the number of layers surrounding the central heat source.

III. Numerical Simulation Results

Photonic Crystal Fibers (PCFs) can be either a hollow core or a solid core. The light guiding mechanism are different in these two types of PCFs. The constituent materials of these fibers can vary depending on their industrial, laboratory, or research applications. Common materials used to form the PCF structure include silica glass, specialty glasses (such as fluoride, chalcogenide, etc.), polymers like PMMA and polycarbonate, and also hybrid and composite materials combining silica with

polymers or nanomaterials to enhance optical and mechanical properties. Among these, silica is the most common material for PCF fabrication, especially in optical communication applications, due to its low loss in the infrared range and its suitability for creating complex structures with numerous air holes.

In addition to air, other substances are also used to fill the holes within photonic crystal fibers. Common hole-filling materials include hydrogen (H_2), nitrogen (N_2), argon (Ar), krypton (Kr), and SF_6 (used for nonlinear and sensing applications). These types of fibers are employed in gas sensing through spectroscopic absorption and for enhancing nonlinear effects (such as Raman scattering). There are also reports of filling holes with solid materials (nanoparticles or polymers), which are primarily for research purposes. Various methods exist for sealing the ends of the fiber to prevent gas leakage from the holes. These include, Physical Sealing of Fiber Ends, such as Thermal Fusion (Heat Fusion): Using heat to collapse and seal the holes at the fiber end. Epoxy or UV-Curable Adhesives, such as Applying specialized glues that cure with heat or UV light to seal the openings. Thin-Film Deposition: Applying thin layers of material to the fiber ends. This includes, Atomic Layer Deposition (ALD). Such as A precise thin-film deposition technique. Polymer Coating: Applying a polymer layer to seal the fiber ends.

In this paper, two structural compositions, air-Si and H2-ZBLAN, are simulated and compared. The aim of this work is to demonstrate why photonic crystal fibers made of the Air-Si combination are used as amplifiers and lasers, while fibers made of H2-ZBLAN are employed in low-power optical applications such as sensors.

The simulation procedure used in this work follows the analytical–numerical method developed in our previous publication [24]. In this method, the photonic crystal fiber (PCF) cladding is divided into radial layers, each composed of 6i identical unit cells in the i-th layer. The thermal resistance of each unit cell is calculated using the relations derived in [24, 25] based on the geometrical configuration and material conductivities of glass and air. The unit-cell resistances within the same layer are combined in parallel, and the layer resistances are connected in series to obtain the total effective thermal resistance of the cladding.

Using the theoretical model presented in this paper, the overall thermal conductivity of the photonic crystal fiber cladding with a honeycomb structure is determined. Three steps are required to achieve the proposal. First, Unit Cell Thermal Conductivity must be determined. Then using Eq. 3, the thermal conductivity calculates in each layer. At the end the effective thermal conductivity of the structure determines in the PCF with the honeycomb structure. The thermal conductivity values for all materials used in this simulation are presented in Table 1.

Table 1. Thermal conductivity coefficients in various materials.

Material	Thermal conductivity (W/m K)
Si	1.37
ZBLAN	0.7
Air	0.026
H_2	0.182

Figure 4 illustrates the variations in the thermal conductivity coefficient of the hole-containing region of the unit cell (the middle region in Figs. 2(a) and 2(b) for different values and $\theta = \frac{\pi}{6}, \frac{\pi}{9}, \frac{\pi}{15}, \frac{\pi}{12}, \frac{\pi}{18}$ of the unit cell, based on the changes in the hole diameter. This is shown for a PCF with two distinct structures. The arrows, directed from left to right in the figure, represent an increasing trend in the Λ values, which range varies from 1 to 19 μm.

As observed in Fig. 4, for all values of *d* and Λ, a set of solutions is plotted for different θ values. These solutions are closely grouped, meaning that rotating the unit cell in the direction of the heat flux has little effect on the thermal conductivity coefficient of the hole-containing region and thus the overall thermal conductivity of the unit cell. For each constant

Λ value, there exists a specific point of d on the graph where the thermal conductivity coefficient for all θ values become the same. This value is approximately 0.5 W/m·K for the Air-Si fiber structure, and approximately 0.28 W/m·K for the H2-ZBLAN fiber structure.

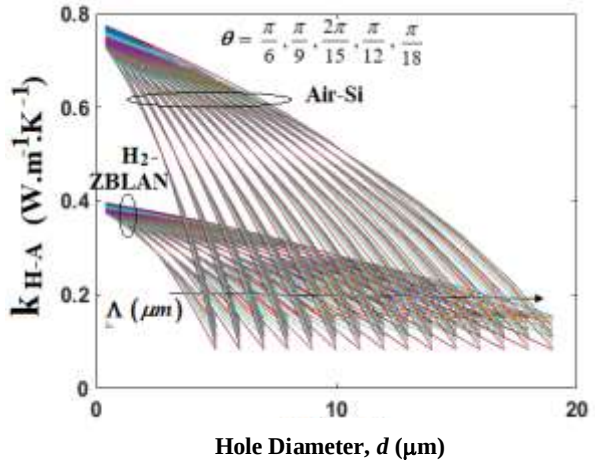

Fig. 4. Thermal conductivity of hole-containing region of unit cell for $\theta = \frac{\pi}{6}, \frac{\pi}{9}, \frac{\pi}{15}, \frac{\pi}{12}, \frac{\pi}{18}$ in different unit cell sizes in honeycomb PCF structure with Air-Si and H2-ZBLAN materials.

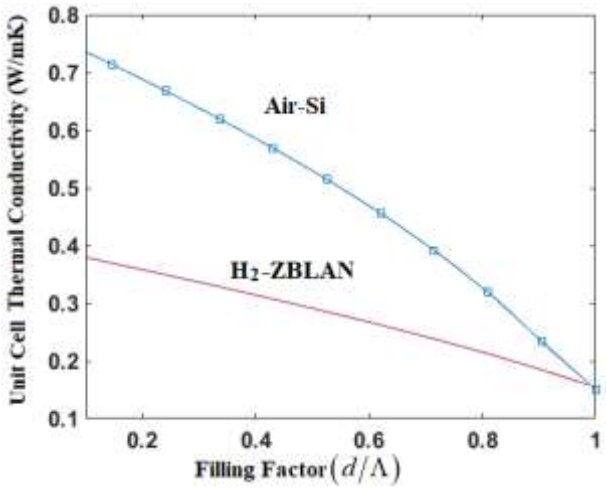

Fig. 5. Unit Cell Thermal Conductivity with respect to filling factor d/Λ for $\theta = \frac{\pi}{6}$.

For any constant Λ, as the hole diameter (d) increases, the thermal conductivity of the hole-containing region decreases. This trend aligns with the increase in gas presence in the hole-containing region and the consequent rise in the thermal resistance of the material. The rate of decrease in thermal conductivity is more rapid for smaller Λ values. The thermal conductivity changes in the hole-containing region of the photonic crystal fiber made from the Air-Si combination range approximately from 0.1 W/m·K to 0.8 W/m·K, while for the fiber made from the H2-ZBLAN combination, this range is also from 0.1 W/m·K to 0.8 W/m·K.

Figure 5 illustrates the variations of the thermal conductivity of Unit Cell with respect to filling factor d/Λ for $\theta = \frac{\pi}{6}$. The Filling Factor represents the ratio of the filled space (e.g., air or H_2) to the total volume of the unit cell. The blue Line shows (Air-Si) unit cell thermal conductivity results.

As observed in this Figure, with an increase in the "Filling Factor" (i.e., an increase in the air content within the cell), the unit cell thermal conductivity gradually decreases, approaching to the thermal conductivity of air. This trend is logical. Even when the Filling Factor reaches near one, the thermal conductivity decreases to approximately 0.15 W/mK but does not become exactly equal to that of air thermal conductivity. This is because the unit cell has a hexagonal shape, and even when the side length of the unit cell equals the diameter of the hole within it, there remains some volume of the unit cell occupied by the solid cell-forming material. The red Line in this figure correspond to the PCF made of (H2-ZBLAN): This line corresponds to a system composed of H2 (hydrogen) and ZBLAN (a type of fluoride glass). In this case, too, with an increase in the "Filling Factor" (i.e., an increase in H2 content), the unit cell thermal conductivity decreases. However, the overall thermal conductivity values for this system are lower than those of the Air-Si system. For example, at a Filling Factor close to 0.1, the thermal conductivity is approximately 0.38 W/mK, and as the Filling Factor increases to 1, this value reaches approximately 0.16 W/mK. This implies that H2-ZBLAN is inherently less thermally conductive compared to Air-Si, or that ZBLAN itself is less conductive than Si. The process of change is the same for the other angles. This figure provides the foundation for subsequent calculations, demonstrating how the material composition and their ratios within the

smallest building block (the unit cell) influence thermal conductivity. For a constant d/Λ by increasing in the 'd' or Λ values, there is no change in the graph. The variations in unit cell thermal conductivity as a function of the filling fraction are solely dependent on the types of the core and hole-filling materials.

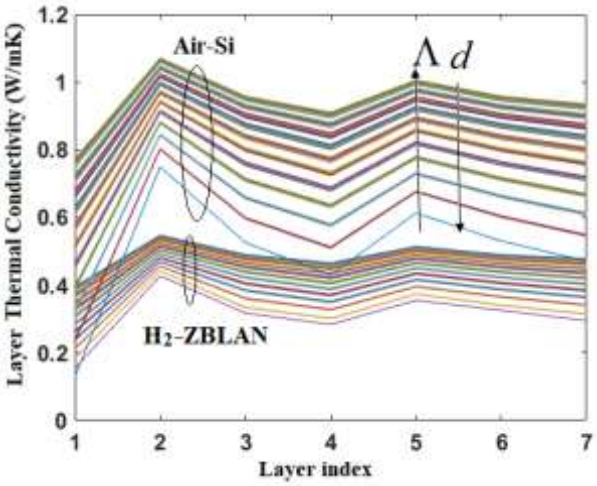

Fig. 6. Layer thermal conductivity as a function of layer number in PCF with honeycomb lattice structure.

Figure 6 illustrates the variation of layer thermal conductivity as a function of layer number. Each group of curves corresponds to a specific combination of materials used in the unit cell and its hollow region. The direction of each arrow indicates the increasing trend of parameters d and Λ. However, despite their concurrent increase, thermal conductivity of layer exhibits opposite behaviors: increasing the unit cell size Λ for constant d cause to enhances the thermal conductivity coefficient of layers, whereas increasing d suppresses it, as reflected by the upward and downward arrows, respectively. In Fig. 5, the unit cell size varies from 5 to 19 micrometers, and the filling fraction ranges from 0.1 to nearly 1. The upper set of curves corresponds to photonic crystal fibers (PCFs) composed of Air-Si. By adjusting d and Λ, the layer thermal conductivity can be tuned between approximately 0.5 and 1 W/m·K**.** As observed in the figure, increasing the number of layers—i.e., increasing the number of unit cells in the thermal resistance network—causes the layer thermal conductivity to approach a constant value. For larger unit cells or larger Λ value, increasing the number of layers beyond seven results in minimal fluctuations in thermal conductivity of layers. In other words, the even or odd number of layers—which determines the proportion of non-hollow unit cells—has diminishing influence on the effective thermal conductivity of layers as the layer count increases. The lower set of curves corresponds to PCFs made of H_2-ZBLAN**.** Although the trend of thermal conductivity variation is similar for fibers with the same geometry but different material compositions, the range of variation is smaller in the H_2-ZBLAN-based PCF, where the thermal conductivities of the two constituent materials are relatively close. In this case, changing the spacing between the hollow regions from 5 to 19 micrometers results in thermal conductivity variations between 0.2 and 0.5 W/m·K, with overall values around or slightly below 0.5 W/m·K**.** Moreover, increasing the number of layers beyond five further reduces the amplitude of these variations, indicating a convergence toward a stable thermal conductivity value.

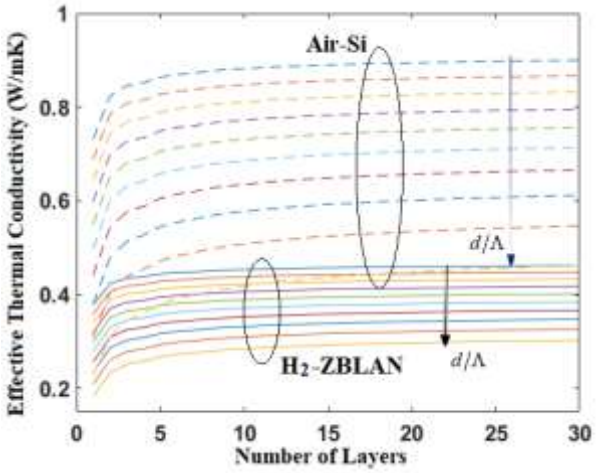

Fig. 7. Effective thermal conductivity of the PCF with Honeycomb lattice structure with respect to Number of layers.

Figure 7 shows total thermal conductivity (W/mK) of PCF with honeycomb lattice structure as a function of the number of layers. The "effective" thermal conductivity represents the final value calculated for the entire structure using the thermal resistance network method (series between layers). The upper set of dashed lines corresponds to the photonic crystal fiber made of Air-Si. Each curve within this set

represents a specific filling fraction, ranging from 0.1 to approximately 1. For a given filling fraction, the effective thermal conductivity increases with the number of layers until it stabilizes at around six layers for the Air-Si composite structure.

Beyond this point, further increasing the number of layers has no significant impact on the thermal conductivity. A higher thermal conductivity value is crucial in fiber amplifiers and lasers, as it facilitates the dissipation of excess heat. In high-power industrial lasers and amplifiers, heat generation is a primary cause of modal instability. As the air filling factor d/Λ increases, the effective thermal conductivity of the Air-Si structure decreases. This is because a higher air content enhances the thermal resistance of the photonic crystal fiber, bringing its effective thermal conductivity closer to that of air.

The lower set of solid lines represents the photonic crystal fiber made of H_2-ZBLAN. As evident from the figure, the effective thermal conductivity for any given air filling fraction is consistently lower than that of the Air-Si fiber. This lower conductivity traps heat within the fiber, hindering its dissipation. Consequently, H_2-ZBLAN photonic crystal fibers are not suitable for fiber amplifiers and lasers but are primarily used in the design and fabrication of fiber-based sensors.

Similar to the Air-Si structure, increasing the air filling factor d/Λ in the H_2-ZBLAN fiber reduces its effective thermal conductivity, approaching that of H_2 gas. Additionally, for the H_2-ZBLAN fiber, increasing the number of layers beyond three does not alter the effective thermal conductivity. Instead, the reflection at the layers and the cladding resistance become the determining factors for optimizing the design of photonic crystal fibers made from this material.

IV. CONCLUSION

This study developed a robust analytical framework to predict the effective thermal conductivity of honeycomb-lattice PCFs, bridging a critical gap between numerical methods and design practicality. The model's key contributions include. Geometric innovation, by resolving the honeycomb structure's dual unit-cell types, the approach outperforms triangular-lattice models, achieving high accuracy in layer-wise conductivity predictions.

Material insights, air-Si PCFs exhibit superior thermal dissipation (0.8 W/m·K at d/Λ =0.1) for high-power applications, while H_2-ZBLAN's lower conductivity (0.38 W/m·K) favors sensor designs by trapping heat.

Design Rules: Convergence occurs at more than 6 layers of Air-Si, and 3 layers of H_2-ZBLAN, with $d/\Lambda > 0.5$ reducing conductivity by 50%, independent of d/Λ ratios.

The present work focuses on developing a new analytical model for estimating the effective thermal conductivity of honeycomb photonic-crystal structures. Direct numerical or experimental validation is not included here because suitable benchmark data are not yet available in the literature, and performing such measurements requires specialized equipment beyond the scope of this theoretical study. However, dimensional analysis and parametric trends confirm that the model produces physically consistent results. This analytical formulation can therefore serve as a foundation for future numerical or experimental studies aimed at validating and further extending the model.

REFERENCES

[1] L.J. Gibson and M.F. Ashby, *Cellular Solids: Structure and Properties*, 2nd Ed., Cambridge University Press, 1999.

[2] H. Wadley, "Multifunctional periodic cellular metals," Philosophical Transactions of the Royal Society A, Vol. 364, no. 1838, pp. 31-68, 2006.

[3] X. Song, S. Hong, J. Wang, X. Zhu, S. Guo, Y. Fu, Y. Yang, M. Yang, W. He, Y. Tang, and B. Gao, "Mechanical properties of a honeycomb structure dispersed with 3D-printed Fe_3O_4 nanomaterials," ACS Omega, Vol. 9, pp. 14287-14296, 2024.

[4] J. W. Hutchinson and Z. Suo, "Mixed mode cracking in layered materials," Adv. Appl. Mech., Vol. 29, pp. 63–191, 1992.

[5] Q. Zhang, X. Yang, P. Li, G. Huang, S. Feng, C. Shen, B. Han, X. Zhang, F. Jin, F. Xu, T. J. Lu, "Bioinspired engineering of honeycomb structure – Using nature to inspire human innovation," Prog. Mater. Sci., Vol. 74, pp. 332-400, Oct. 2015.

[6] H.M. Hameed, H. M. Hasan, "Exploring honeycomb structures: A review of their types, general applications, and role in vibration damping and structural stability," Structures, Vol. 76, pp. 108837(1-42), Jun. 2025.

[7] A. Evans, J. Hutchinson, and M. Ashby, "Multifunctionality of cellular metal systems," Prog. Mater. Sci., Vol. 43, pp. 171–221, 1999.

[8] H. Yin, W. Zhang, L. Zhu, F. Meng, J. Liu, G. Wen, "Review on lattice structures for energy absorption properties," Compos. Struct., Vol. 304, no. 1, pp. 116397(1-40), Jan. 2023.

[9] T. Goldmann, W.-C. Huang, S. Rzepa, J. Džugan, R. Sedláček, and M. Daniel, "Additive manufacturing of honeycomb lattice structure—From theoretical models to polymer and metal products," Materials, Vol. 15, no. 5, pp. 1838(1-11), 2022.

[10] A.P. Roberts and E.J. Garboczi, "Elastic properties of model porous ceramics," J. Am. Ceramic Soc., Vol. 83, no. 12, pp. 3041–3048, 2000.

[11] Q. Zhang, X. Xu, H. Li, G. Xiong, H. Hu, and T.S. Fisher, "Mechanically robust honeycomb graphene aerogel multifunctional polymer composites," Carbon, Vol. 93, pp. 659-670, Nov. 2015.

[12] K.P. Gadkaree, "Carbon honeycomb structures for adsorption applications," Carbon, Vol. 36, no. 7-8, pp. 981-989, 1998.

[13] D. Köllner, S. Simon, S. Niedermeyer, I. Spath, E. Wolf, K. Kakimoto, and T. Fey, "Relation between structure, mechanical and piezoelectric properties in cellular ceramic auxetic and honeycomb structures," Adv. Eng. Mater., Vol. 25, no. 3, pp. 2201387–2201394, Feb. 2023.

[14] A. Halder, M.R. Tanshen, M.A. Hossain, M.S. Akter, and M.A. Sikdar, "Tailored dispersion and nonlinear effects in flint glass honeycomb PCF for optical communication," J. Opt. Photon. Res., Vol. 1, pp. 43–49, 2024,

[15] M. Makwana, R. Wiltshaw, S. Guenneau, and R. Craster, "Hybrid topological-photonic localization in honeycomb lattice photonic crystal fibers," Opt. Express, Vol. 28, no. 21, pp. 30871–30885, Oct. 2020.

[16] K.R. Hansen, T.T. Alkeskjold, J. Broeng, and J. Lægsgaard, "Thermo-optical effects in high-power Ytterbium-doped fiber amplifiers," Opt. Express, Vol. 19, pp. 23 965–23 980, 2011.

[17] M. Zeeshan, M. Ali, A.S. Anjum, and Y. Nawab, "Optimization of mechanical/thermal properties of glass/flax/waste cotton fiber reinforced composites," J. Compos. Mater., Vol. 51, pp. 768–787, 2021.

[18] K. Pietrak and T.S. Wiśniewski, "A review of models for effective thermal conductivity of composite materials," J. Power Technol., Vol. 95, pp. 14–24, 2015

[19] F. Pascal, "Numerical calculations of the thermal conductivities of composites: a 2-D model," Geophys. J. Int., Vol. 118, no. 3, pp. 623–635, 1994.

[20] W. Chen, "Numerical estimation of effective thermal conductivity of cement-based materials with pore structure reconstruction," Constr. Build. Mater., Vol. 435, pp. 295-314, 2024,

[21] B. Ghanbarian and H. Daigle "Thermal conductivity in porous media: percolation-based effective-medium approximation," Water Resour. Res., Vol. 52, pp. 295–314, 2016.

[22] X. Cheng and J. Xu, "Thermal and thermal-optical effects in high-power photonic crystal fiber lasers," Opt. Eng., Vol. 45, pp. 124204(1-5), 2006.

[23] M. Karimi, "Theoretical study of hole structure and core size on the gap-map of hollow core photonic crystal fiber," Sci. J. Appl. Electromagn., Vol. 11, pp. 95-105, 2023.

[24] M. Karimi, "Theoretical model to determine the effective thermal conductivity coefficient of first clad region in photonic crystal fiber with the hexagonal structure," Thermal Sci. Eng. Prog., Vol. 19, pp. 100574(1-14), 2020.

[25] M. Karimi, "Analytical Model to Determine Thermal Conductivity Coefficient of Honeycomb Structure with Heat Flux Distribution Outside the Central Cylindrical Axis", Mechanical Engineering, Sharif. J., in Press, Vol. 25, pp. 111-123, 2025.

Maryam Karimi received her B.Sc. and M.Sc. degrees in Physics from K. N. Toosi University of Technology and Tarbiat Modares University, Tehran, Iran, in 1999 and 2002, respectively. She obtained her Ph.D. in Physics (Optics) from Razi University in 2010. From 1999 to 2003, she worked as a research member at the Iran Telecommunication Research Center (ITRC). Between 2010 and 2012, she joined the National Fusion Plan at the Plasma and Nuclear Fusion Research School. Dr. Karimi is currently a faculty member of the Photonic and Quantum Technology Research School at the Nuclear Science and Technology Research Institute (NSTRI). She has published more than 80 papers in peer-reviewed journals and conference proceedings and has authored two books. Her research interests include optical fiber instruments such as photonic crystal fiber sensors, optical fiber lasers and amplifiers, nonlinear optical effects, light sources for quantum communication, and laser dielectric accelerators.